

GA-A24767

**STRUCTURAL UPGRADE OF IN-VESSEL
CONTROL COIL ON DIII-D**

by

P.M. ANDERSON, A.G. KELLMAN, E.E. REIS

AUGUST 2004



DISCLAIMER

This report was prepared as an account of work sponsored by an agency of the United States Government. Neither the United States Government nor any agency thereof, nor any of their employees, makes any warranty, express or implied, or assumes any legal liability or responsibility for the accuracy, completeness, or usefulness of any information, apparatus, product, or process disclosed, or represents that its use would not infringe privately owned rights. Reference herein to any specific commercial product, process, or service by trade name, trademark, manufacturer, or otherwise, does not necessarily constitute or imply its endorsement, recommendation, or favoring by the United States Government or any agency thereof. The views and opinions of authors expressed herein do not necessarily state or reflect those of the United States Government or any agency thereof.

GA-A24767

STRUCTURAL UPGRADE OF IN-VESSEL CONTROL COIL ON DIII-D

by

P.M. ANDERSON, A.G. KELLMAN, E.E. REIS

This is a preprint of a paper to be presented at the 23rd Symposium on Fusion Technology, Venice, Italy, September 20-24, 2004 and to be printed in Fusion Engineering and Design.

Work supported by
the U.S. Department of Energy
under DE-FC02-04ER54698

GENERAL ATOMICS PROJECT 30200
AUGUST 2004



ABSTRACT

For most of the 2003 operations campaign, the DIII-D tokamak successfully operated 12 new in-vessel outer wall-mounted control coils (I-coils). The single turn, rectangular shape saddle coils are mounted in two horizontal arrays of six coils each. The coils were used for many experiments such as suppression of the resistive wall mode, an instability that limits the plasma performance at high beta, for correction of magnetic field imperfections and for creation of an ergodic edge magnetic field for the suppression of edge localized modes (ELMS). During operation at currents of 4.5 kA, at a constant frequency of 100 Hz, one of these coils developed a leak through the stainless barrier that separates the nitrogen blanketed, insulated conductor from vessel vacuum. A pair of coils was taken out of operation for the remainder of the campaign greatly limiting the usefulness of the remaining 10 coils. This paper describes the failure investigation, analysis, design, repair, system testing and new interlocks of the repaired system for these coils that are getting significant use in the 2004 campaign.

1. BACKGROUND, FAILURE EVENT AND RECOVERY

The design of the 12-coil in-vessel I-coil set was adapted from the two prototypes installed in 2001 [1]. Minor changes were incorporated to improve fabrication and assembly issues [2]. Figure 1 shows the arrangement of the 12 single turn coils inside the toroidal vacuum vessel. Pairs of coil leads exit from six ports that are of three different designs. Each port design requires coaxial lead conductors of different length and geometry. The key design requirements for the single-turn coil system are steady-state operation in the 2.2 T toroidal magnetic field, with currents of up to 7 kA at frequencies from dc to 1000 Hz, and being able to fit in the space behind the existing graphite wall tiles for protection from plasma contact.

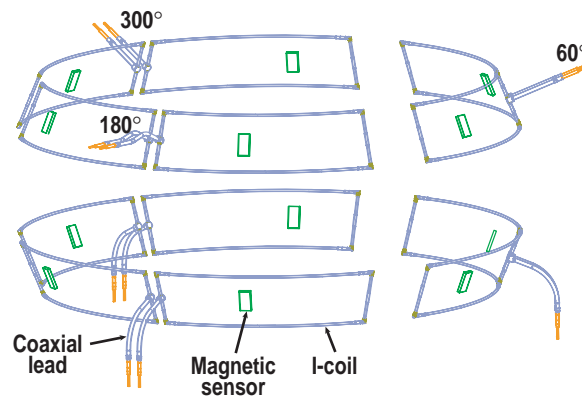


Fig. 1. Spatial location of 12 I-coils in DIII-D. Note magnetic feedback sensors and three types of coaxial leads.

Figure 2 shows the two prototype coils that were installed in DIII-D in 2001. The single coil turn have a conductor length of 5 m and an area of 1 m². In order to minimize error fields and electromagnetic forces, the radially oriented power and cooling water feeds are coaxial and extend out from the vessel surface to near the outer edge of the toroidal field (TF) coils. The I-coils are shielded from the plasma by the graphite tiles that are shown partially installed.

One of the 12 I-coils developed a leak through its vacuum boundary sheath during the first attempt to operate the coils at 4.5 kA, 100 Hz in a 1.6 Tesla TF with the coils connected in a configuration to produce a N=3 field at the plasma edge. The plasma edge field structure for the frequently used N=1 and N=3 modes is shown in Fig. 3. DIII-D is capable of a 2.2 Tesla TF. An explanation of forces applied to the coaxial leads is given in Section 2.



Fig. 2. Installation of two prototype I-coils in DIII-D, October 2001.

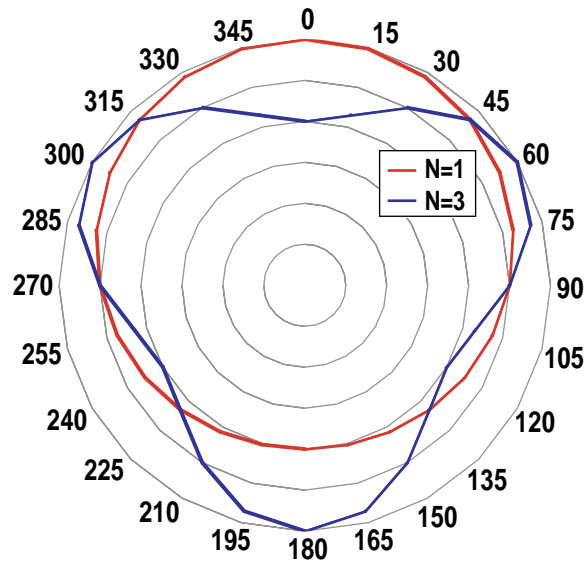


Fig. 3. Shape of N=1 and N=3 radial fields from the I-coils. Fields may be stationary or rotating. The fields from the lower and upper sets of coils can be in phase or out of phase. The magnitude of the radial field (arbitrary) is plotted versus toroidal angle.

The two I-coil leads that share a vessel port are attached to a right hand coil and a left hand coil. The center conductor in the coax bends upward for all coils above mid-plane and then turns to form loops that rotate either clockwise or counterclockwise. Since the coils are located on 60° toroidal spacing, current flow into both center conductors of a feed point form opposite magnetic fields and this pattern, repeated three times, produces the N=3 structure as shown in Fig. 3. For N=1, the coil spacing of 60° requires a field phase shift of 60° that is produced by a current phase shift of 120° between the two center conductors within a port.

Repetitive forces, described in Section 2, applied at a frequency near the first natural frequency of the lead, can produce the relatively large vertical deflections that cracked the

stainless sheath after about 100 stress cycles. The crack allowed pressurized nitrogen, at 1.3 bar absolute, to leak into the vessel terminating the plasma discharge. The dry nitrogen gas surrounds the copper conductor and polyamide insulator to prevent oxidization of the copper and polyamide during vessel baking at 350°C. In addition to the leak, review of tokamak data revealed unusual, although acceptable, vertical motion of the DIII-D vessel during the failure of about ± 0.2 mm at 100 Hz. Although this deflection is about 10% of that developed at 21 Hz during strong plasma disruptions, it does produce higher accelerations than the disruptions.

A roughing pump was connected to the nitrogen supply port on the damaged I-coil pair to prevent leakage of air into the vessel and to permit continued plasma operations without the use of this pair. A successful hi pot test of 1 kV between the coil and ground assured the coil was not shorted. Plasma operations were resumed within a day allowing operation of the remaining 10 I-coils. However, there was little, if any, use of the unbalanced 10-coil set.

Subsequent inspection of the leaking coil, aided by a magnifying glass, detected a horizontal crack across the inward facing surface of the upper 19 mm transition sleeve near its attachment to the stiff 63 mm diameter coaxial assembly. The neighbor coil in the same port was also found to have a crack indication but no leak. This failed set of coil leads were the longest used in the I-coil system and have a common, relatively low, first natural frequency. No cracks were seen in the other 10 coils.

2. FORCES APPLIED TO I-COIL COAXIAL LEADS

All the coaxial coil leads are supported inside the vessel by the single vertical conductor that is shown in Fig. 2. The pair of leads within a port is further restrained to the neighbor by a horizontal brace called the handcuff. The ends of the handcuff are attached at the edge of the port to a radially flexible member designed to allow radial freedom for coaxial lead growth during vessel baking to 350°C. The support at the vacuum vessel flange uses a thin wall sleeve between the lead and the flange. This welded sleeve is rigid axially but has some flexibility for moment restraint. There are no bellows in this design.

Alternating current in the I-coil system produces cyclic forces in the leads that is likely due to two sources:

1. The force produced from radial directed $I \times B$ forces in the vertical single conductors inside the vessel that attach to the coaxial leads as shown in Fig. 2. This portion of the vertical conductor passes over the port aperture and is structurally supported at the top or bottom of the port aperture and at the coaxial lead. The coax leads in the 180R+1 port where the damage occurred, as shown in Figs. 1 and 2, have vertical bends. A significant portion of the alternating radial forces of 6200 nt generated in the vertical conductor for full TF-coil and I-coil currents is applied to vessel end of the bent coaxial lead in the 180R+1 port, resulting in vertical or lateral deflections of the coax leads.
2. The force produced outside the vessel, by $I \times B$ forces, generated in the unbalanced transition between quadrupoled feed cables and the coaxial lead immediately outside the vessel port. The TF is dominant in this area and, although this produces a primarily radial force of 50 nt on the coil lead that is then transferred to the port, the vertical and lateral forces developed are significant and about half of the radial force.

The current phase in the pair of ex-vessel leads can double the force applied to the port or nearly cancel the force depending on the N number. Radial forces ($I_{\text{poloidal}} \times B_{\text{toroidal}}$) on the in-vessel vertical conductors are in phase with each other and, therefore, the radial forces are additive for the N=3 connection as compared to the nearly canceling 120° current phase shift that occurs with the N=1 connection. Strain gages installed during the N=1, but not the N=3, testing showed horizontal strains on the 180R+1 lead that are likely produced by radial push-pull forces acting on the two vertical conductors with their handcuff connection.

3. FEA STRUCTURAL MODELING

The horizontal cracks were consistent with the theory of resonant vertical vibration of the coaxial section of the I-coil leads inside the port. Analysis and testing of the prototype coils had neglected deflection monitoring of the leads since the coaxial design assured no net $I \times B$ forces. Earlier tests emphasized the single conductor portion of the coil since $I \times B$ forces were clearly present and significant. The single conductor coil sheath is attached rigidly to the vessel every 15 cm as seen in Fig. 2. The single conductor far away from the coaxial lead had been instrumented with field compensated strain gages during in-air $I \times B$ testing of the prototypes including I-coil frequency sweeps. The strain gage signals had not indicated any resonances to 1000 Hz. All prototype testing was done in the N=1 configuration.

Initial FEA modeling of the vessel port, coaxial lead and vertical conductors of the coil, as shown in Fig. 4(a), predicted a vertical mode of the lead at 125 Hz. This model is constructed from a number of elements with a combined stiffness that includes the copper, polyamide and stainless steel and a combined mass that includes those materials plus cooling water. The ex-vessel portion of the coaxial lead and its transition into quadrupole cabling was not modeled. At resonance, theoretical system deflection of an ideal spring-mass system is limited only by damping. Early modeling was done with 2% damping but cantilever beam decay testing indicated 4% damping. After the vessel was opened for in-vessel work, dynamic testing of the leads at this port (180R+1) indicated a first natural frequency of 110 Hz based on accelerometer output. The FEA model was updated to include the repair elements and is shown in Fig. 4(b).

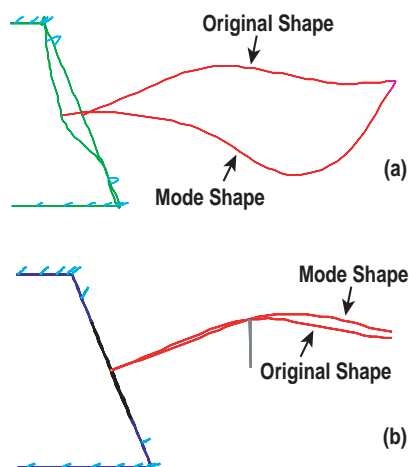


Fig. 4. Mode shapes of 180R+1 I-coil lead at first vertical resonance for (a) 2002 installation and (b) 2004 with vertical stiffness and mid-length support. The calculated vertical deflection at resonance has been reduced from (a) 8 mm at 110 Hz to (b) 0.5 mm at 365 Hz.

4. REPAIR APPROACH

Since there was no detectable damage to the I-coil electrical insulation, in-situ repair of the cracked coil was planned. Three different styles of coaxial leads are shown in Fig. 1. FEA modeling of the failed lead indicated that the coaxial conductor must have flexed about ± 9 mm vertically at its mid-length in order to develop a crack within 100 cycles. The required force to develop this deflection could be produced in the unsupported sections of the single conductor at the vessel ports if the driving force were at the resonance of the coaxial lead. A mid-length location on the lead was chosen for the installation of a support to form a vibration node and significantly increase the first natural frequency of the lead at the 180R+1 port location. This added support is shown in Figs. 5 and 6. A split sleeve, also shown in Figs. 5 and 6, was welded in place over both single conductors for this coil to seal the leak and to smooth the stiffness change from the coax to the single conductor. The two other upper ports at toroidal locations of 60° and 300° have shorter, straight coaxial leads with a fundamental vertical frequency around 300 Hz which was considered to be acceptably high and, therefore, required no mid-length support. These coils were also modified with single conductor stiffeners at the connection to the coaxial lead. The three sets of coils on the lower half of the tokamak have identical feeds at 60° , 180° , and 300° . These leads are of intermediate length with a single bend and required both a mid-length support and single conductor stiffeners at the connection to the coaxial lead.

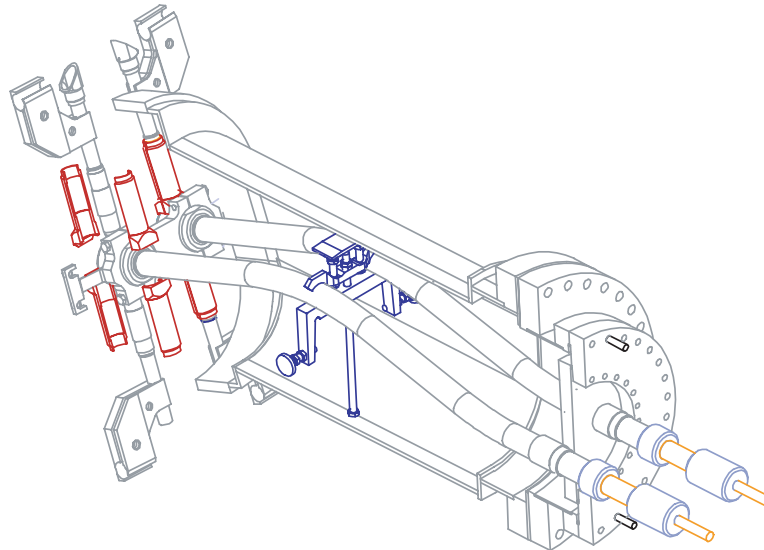


Fig. 5. Split sleeve and lead stabilization hardware installed to repair failed I-coil at 180R+1 port. Blue parts are the mid-length lead support. Red parts are the split sleeve assemblies to seal the leak and increase stiffness.

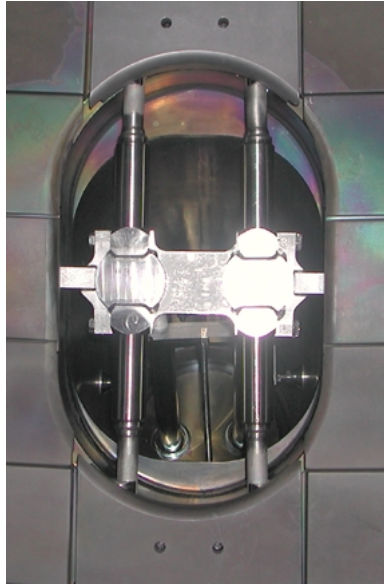


Fig. 6. Repaired I-coils at 180R+1 port.

The construction of the coil starting from the outside is generally 0.8 mm thick stainless steel tube wall, 1.5 mm thick polyamide insulation and 14 mm diameter hollow copper conductor. Welding directly on the stainless overheats and chars the polyamide. The coil has specific areas designed for welding and the split sleeves were circumferentially welded in this area. The seam welds between the halves did not contact the underlying stainless and heating was not an issue. Welding directly to the stainless cylinder at the transition of the single coil conductor to coaxial feed is allowed due to the thick wall construction of the cylinder. Practice welds were developed on sample parts attached to a vacuum vessel wall mockup in order to assure welder access. A mechanical loading device measured the radial stiffness of the original and reinforced vertical conductors in the mockup. The stiffness increase was about 250%. This measured stiffness was used in the FEA for natural frequency determination. It was also used in analysis to assure acceptable compliance of the system during vessel baking.

The 10 coils without visible cracks were reinforced with two four-piece welded cradle stiffener assembly for each conductor. These were easier to weld and, unlike the split sleeve, did not require graphite tile removal and replacement.

During the modification of the coil leads, natural frequency of each type of lead was measured at each repair step in order to tune the FEA model to the measured frequencies. This measurement was made by impacting the lead and monitoring the response from an accelerometer mounted on the coax lead. The addition of both the vertical split sleeves and the lead stabilizer increased the measured natural frequency of the failed I-coil from 110 to 365 Hz.

5. TESTING AND DATA EVALUATION

A satisfactory repair was confirmed by in situ testing of the upgraded I-coils with applied fields prior to vessel closure. Temporary installation of field-tolerant strain gages on each of the three types of I-coil leads was used during these tests. The lead at 180R+1 port, which had cracked through, was equipped with both a top and a side strain gage to monitor both vertical and horizontal strains. Leads in two other ports, 300R+1 and 180R-1, were equipped with strain gages to monitor only vertical strain. In addition, there were three permanent port deflection monitors installed to monitor vertical deflections of the outer end of the ports at 180R+1, 300R+1 and 180R-1. The 180R+1 port also had a deflection monitor to measure radial motion of the port. The plan was to correlate lead strains with port deflections and, if necessary, base interlocked limits for future operation on measured port deflections. The test plan required frequency scanning of I-coil currents over the range of dc to 1000 Hz in several 6 s shots. The magnetic field was to be developed using the TF for a $I \times B$ of about 30% of the maximum capability for the N=3 configuration. This identified resonances and predicted if acceptable strains would be produced in full $I \times B$ shots. Higher $I \times B$ conditions were tested as desired. Two N=1 shots were done to understand the difference due to different N configurations.

Test results showed that strain gage output was generally below expectations. Updating the analysis from 2% damping to 4% damping brought the analysis results into better agreement with the test results and increased the calculated safety margin. The strain gages showed the vertical first natural frequencies were all above 300 Hz for the three I-coils monitored. There were many resonances detected on the port displacement monitors. Most of these were later shown to be resonances of the displacement monitors targets and not of the ports. These targets were later determined to have resonances in the range of 50 to 300 Hz. Discounting the sensor resonances, there remained unexplained port resonances in the 80 to 100 Hz range. The N=1 testing revealed significant, although acceptable, horizontal strain in the 180R+1 coil lead. This testing confirmed that the in-vessel modifications had stabilized the leads and corrected the conditions that produced the cracked sleeve but that port vibrations caused by I-coil operation at specific frequencies required additional evaluation.

A second test was done after stiffening the port displacement sensor targets. The radial port deflection sensor on the 180R+1 port, was reoriented to measure horizontal traverse, or tangential port deflection. This test eliminated the confusion of port deflection sensor resonances but sensors on the lower ports still indicated significant vertical deflections around 85 Hz. This deflection was nonsymmetrical indicating that a gap was likely developing in a bolted joint during half of each load cycle. Operation of the I-coils is ongoing during 2004 with lower current limits enforced for operation in the 50 to 120 Hz range.

6. PROTECTIVE INTERLOCKS

Based on the results of the tests with improved port displacement sensors, it was evident that there were real $I \times B$ force driven vibrations of the ports at 180R+1 and the three R-1 ports. Although there has been no noticeable damage, the vibrations on the lower ports have loosened local fasteners, nitrogen system tube fittings, and driven vertical vibrations of the vacuum vessel. Since the earlier testing with strain gages on the in-vessel leads showed well-stabilized coaxial leads, it was assumed that the forces on the ports were being developed outside the vessel at the cable connection to the coaxial leads. These forces are described in Section 7. To prevent excessive vibrations, interlocks were developed using the port deflection sensors to shut down the I-coil power supplies when the port deflections indicate stresses exceeding the endurance limit of the Inconel material of the vessel and ports. The trip-point is conservatively set at 0.6 mm for vertical and lateral deflections. These interlocks were verified to be operational but as yet have not been triggered. Administrative limits have also been applied to operation of the I-coil at frequencies in the 50 to 120 Hz range.

7. ANALYSIS OF EX-VESSEL FORCES DUE TO UNBALANCED CURRENT PATHS

The lower six I-coil leads exit the vessel through three identical vacuum pumping ports that were modified in place (2002) to allow the leads to exit through the floor of these ports. The transition from coax to quadrupole cabling for these coils is located in a lower TF region than the corresponding upper coils and they therefore experience lower $I \times B$ forces. However, the structural support of the transition region for the lower coils is inherently less robust than the upper coils due to spatial constraints shown in Fig. 7. The footprint of the structural support bolted to the modified port, which is not visible in Fig. 7, is relatively small. The port deflection sensor, that is mounted to the bolted structure, displays nonsymmetrical deflections indicating that the preload in one of two attachment bolts is being exceeded and causing a gap to form in the joint during vertical vibrations of the lead.



Fig. 7. Electrical power and fluid connections to a pair of lower I-coils. The transition between coaxial lead and quadrupoled power cable produces some uncancelled $I \times B$ forces.

A detailed analysis [3] of the $I \times B$ forces was performed for this transition area to determine the forces generated by the unbalanced current path. Figure 8 shows the magnetic field from the TF coil set. Analysis was also done for the poloidal coil magnetic field that produces lower forces than the TF. Forces were calculated for the points along the unbalanced I-coil current flowing in the copper plate that connects the inner coax conductor to the power cables. This path is shown in Fig. 9(a) along with a proposed modification to the path. These forces are shown for one coil in Fig. 9(b) for a 7 kA I-coil current and a 2.2 T TF, sum to 28 nt toroidally and 58 nt in the radial-vertical plane that contributes to flange liftoff. The net force applied to the port, depending on the N=1 or N=3 connection, is either combined with or nearly cancels those produced in the neighbor coil lead transition.

By redesigning the copper plate to the alternate path shown in Fig. 9(a), these forces are reduced by 30%.

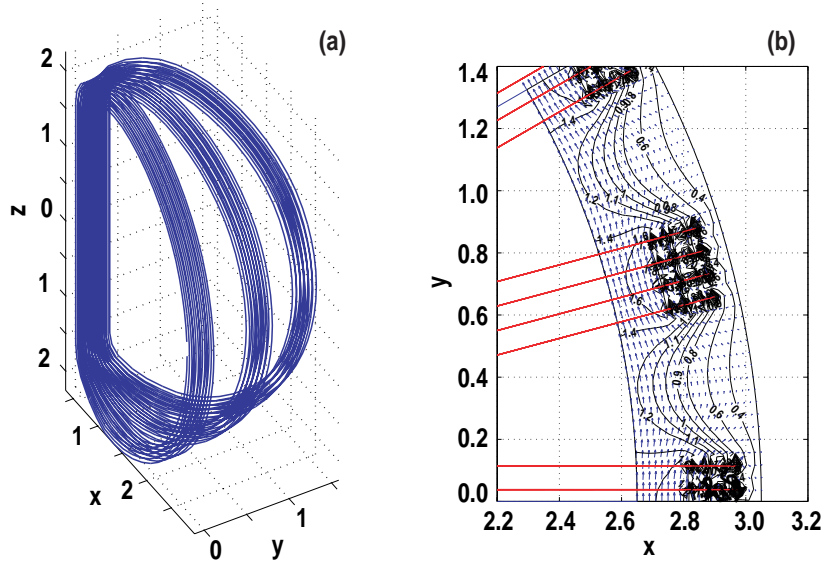


Fig. 8. Magnetic field due to 2.2 T TF at DIII-D. (a) 3-D schematic of toroidal field generating currents. (b) Horizontal cross section of field contours at mid-elevation. Dimensions in meters.

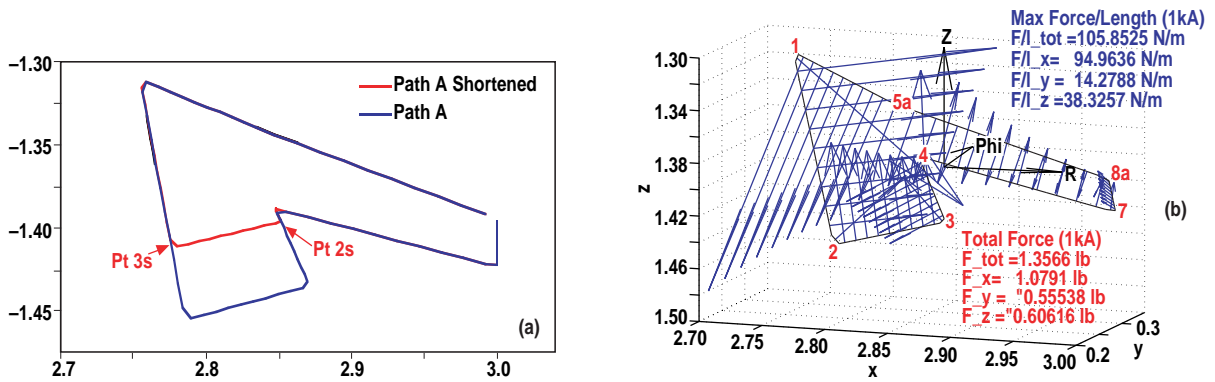


Fig. 9. (a) Path of unbalanced I-coil current in copper transition plate for lower coils. The red line indicates a path reduction of replacement part to reduce $I \times B$ forces by 30%. (b) Force generated in copper transition plate due to $I \times B$.

An upgrade is scheduled for installation in September 2004 to (1) reduce the applied loads due to unbalanced currents by 30% to the lower port leads by redesign of the copper bus plate, and (2) increase the natural frequency of the I-coil lead supports for the lower ports and improve the attachment fasteners to prevent flange liftoff. This upgrade is expected to allow unrestricted operation of the I-coils throughout the design range of 7 kA, 0 to 1000 Hz.

8. CONCLUSIONS

Draw the following conclusions from the last 3 years of I-coil development and operation:

- In 2001, confidence was developed for the installation techniques and from the operation of two prototype coils. However, the testing was incomplete due to the absence of high current frequency sweeps at maximum TF for both N=1 or N=3 connections. It is important to thoroughly test prototypes.
- Initially, the low level of force calculated for the external imbalance was believed to be insignificant. Once this system was available, however, scientists developed an expanded set of experiments with currents at frequencies that could couple to the natural frequency of system hardware. We needed to analyze the systems for resonant frequencies.
- Large changes in stiffness in a mechanical system can concentrate flexure in localized areas. It is best to avoid step changes in stiffness in systems with dynamic loads.

REFERENCES

- [1] P.M. Anderson, C.B. Baxi, A.G. Kellman, E.E. Reis, and J.I. Robinson, Design, fabrication, installation and testing of in-vessel control coils for DIII-D, Proc. 22nd Symp. on Fusion Technology, Helsinki, 2002, to be published in Fusion Engineering and Design.
- [2] P.M. Anderson, C.B. Baxi, A.G. Kellman, and E.E. Reis, Design, fabrication, installation, testing and initial results of in-vessel control coils for DIII-D,” Proc. 20th IEEE/NPSS Symp. on Fusion Engineering, San Diego, 2003, to be published.
- [3] GA memo, J. Leuer to P. Anderson, DIII-D coil fields and forces at the lower I-coil to bus joint, April 30, 2004.

ACKNOWLEDGMENT

This work was supported by the U.S. Department of Energy under DE-FC02-04ER54698.